New Journal of Physics
An Institute of Physics and Deutsche Physikalische Gesellschaft Journal

Localization behaviour in a phenomenological model of three-dimensional knots

Ralf Metzler
NORDITA, Blegdamsvej 17, DK-2100 Copenhagen Ø, Denmark
and
Department of Physics, Massachusetts Institute of Technology,
77 Massachusetts Avenue, Cambridge, MA 02139, USA
E-mail: metz@nordita.dk

New Journal of Physics **4** (2002) 91.1–91.10 (http://www.njp.org/)
Received 26 July 2002
Published 12 November 2002

Abstract. We propose to model three-dimensional (3D) knots as effective vertex networks with vanishing topological exponents to study their equilibrium behaviour. This model is self-consistent and predicts weak localization in knots with up to five essential crossings. The resulting localization exponent for the 3D trefoil is in numerical agreement with a recent simulation study. In more complex knots, however, delocalization is expected. It is shown that this approach corresponds to the decomposition of the knot into C coupled loops of variable size, where C is the number of essential crossings.

1. Introduction

During the polymerization of a long closed chain, freely floating in a solvent, a knot is almost certainly created, i.e. the topology of the final ring polymer differs from that of the simply connected unknot $\emptyset$. Originally conjectured by Frisch, Wassermann and Delbrück [1], it was shown for closed self-avoiding chains more recently that the probability $p(\emptyset)$ of finding a ring polymer with the topology of the unknot decays exponentially with the number N of monomers: $p(\emptyset) \propto \mathrm{e}^{-N/N_0}$ [2]–[4].

The likelihood of knottedness of polymer chains has a profound impact in biology and chemistry. For instance, the permanent entanglements in naturally occurring knotted DNA impede the separation of the two strands of the double helix, and therefore replication and transcription [5, 6]. Specialized enzymes (topoisomerases) are necessary to actively reduce the knottedness of DNA under energy consumption from ATP [5, 6]. The specific operation of these enzymes requires an accurate detection mechanism of knottedness. The existing scenarios for such a mechanism, based on increased bending or decreased waiting periods between collision

1367-2630/02/000091+10$30.00

events between different portions of the DNA in the presence of a knot [7] have been shown to explain the working efficiency of topoisomerases for DNA chains, which are not too long in comparison with the persistence length ℓ_p of the DNA chain. For much longer chains, an additional mechanism is necessary to account for the accuracy of topoisomerases; a plausible explanation may be a (partial) localization of the knotted chain due to thermal fluctuations, i.e. a segregation into a simply connected part and another one containing all topological entanglements. Such a (partial) localization would create bending- or collision-enriched zones and therefore enhance correct detection through the enzymes. Note that in the emanating field of topological chemistry [8], similar entropy-driven localization properties may be employed to create novel designer molecules and materials [9].

Apart from this biophysical motivation, it is a key issue in the understanding of knotted polymers to determine the degree of localization, i.e. the extent of the aforementioned segregation of all non-trivial topological entanglements into a small portion of the knot of length ℓ, from a simply connected structure of length $L - \ell$†. For 2D self-avoiding walks with oriented over- and underpassings, the prime components of a knot become strongly localized, and to leading order behave like point-like objects on the fringe of a simply connected ring polymer [11]. Flat knots, obtained by pressing a 3D knot against a wall by an external force, localize in a *hierarchy* of different contractions of the original configuration [12]. In particular, the gyration radius R_g of such 2D knots is, to leading order, independent of the knot type [11, 12].

For 3D knots, no such rigorous treatment of the localization problem is known. The difficulty arises from the fact that the calculation of statistical properties of a knotted polymer chain in three dimensions requires sampling over the configuration space without changing the topology of the knot. Knot theory provides powerful tools for distinguishing and classifying knots by means of invariants, for example, knot polynomials [13]. However, these methods are hard to implement analytically, and they are based on the *projection* of a given 3D knot onto a 2D plane, which is then further analysed by Reidemeister moves [13]. Although quite successful in classifying knots *per se*, such projections are not directly suitable for evaluating statistical properties, since they may disguise certain symmetries of the knot visible only in the 3D space. In fact, the permanent entanglements in knots effectively reduce the accessible volume in configuration space and cannot be phrased in a Hamiltonian form. The interplay between topological constraints and fluctuations can be studied analytically in 'slip-linked' chains, so-called paraknots [14]. For real 3D knots, one can only retreat to simulations studies and phenomenological models. By Monte Carlo simulations of chains of equal length L, Quake obtained $R_g^2 \sim A(C)L^{2\nu}$, which contains a knot-type sensitive prefactor scaling as $A(C) \sim C^{1/3-\nu}$ with the number C of essential crossings ($\nu = 0.588$ is the swelling exponent) [15]. This dependence on the knot type actually occurs qualitatively in DNA electrophoresis motility studies [16]. The scaling behaviour of $A(C)$ corresponds to the assumption that the knot can be decomposed into C self-avoiding, *non-interacting rings of equal length* L/C, i.e. that the knot is completely delocalized [15]. An analogous result was obtained by Grosberg *et al* [17] from an inflated sausage model. In contrast, a number of simulations studies may indicate that these are finite size manifestations: Katritch *et al* [10] obtained that the size distribution of the knot region is strongly peaked for relatively small ℓ; Janse van Rensburg and Whittington [18], and Orlandini *et al* [19] found for knots with prime components of up to six crossings that in the $L \to \infty$ limit the knot region for each prime

† To actually determine and measure the size ℓ in simulations studies in three dimensions turns out to be problematic; compare, for example, [10].

component is point-like. Remarkably, the localization of (simple) knots can also be recovered in a certain limit of the inflated sausage model discussed by Grosberg *et al* [17], see also [4].

2. Effective knot-graphs

Here we propose a self-consistent map of 3D knots C_m on effective vertex networks, which we call *knot-graphs* $\mathcal{G}(C)$†. For these, we are able to determine the associated number of configurations from which, in turn, the localization properties can be deduced. This modelling is based on the scaling theory for arbitrary polymer networks consisting of self-avoiding chains formulated by Duplantier [20]. Excluded volume effects are not considered, and it is assumed throughout that all segments within a knot-graph are much longer than the persistence length of the chain, i.e. fully flexible.

As in our previous studies of flat knots and paraknots [12, 14] we use the *a priori* assumption that the knot is localized and check for the self-consistency of this assumption. To this end, we assume, *a priori*, that the knot is localized in the sense that all topological entanglements which distinguish the knot C_m from the unknot $\emptyset$ are localized within a certain portion ℓ of the chain, the knot region, leaving its complement of size $L - \ell$ simply connected. The assumed localization implies that the mean size of the knot region $\langle\ell\rangle$‡ is small in comparison with the overall size of the chain L, i.e. $\langle\ell\rangle/L \to 0$ in the long-chain limit we are working in. The latter statement is equivalent to requiring that in the distribution $p(\ell) \sim \ell^{-c}$ of the length ℓ of the knot region the exponent $c > 1$.

If localization in this sense prevails, we make the second assumption which presumes that the number of degrees of freedom ω_{C_m} of a knot C_m is approximately given by the number of degrees of freedom of the corresponding knot-graph $\mathcal{G}(C)$, $\omega_{C_m} \approx \omega_{\mathcal{G}(C)}$, the latter being defined as follows. Consider a given knot projection [13], i.e. the projection of a knot onto a plane such that it corresponds to the configuration with the minimum number of crossings, as shown in figure 1. These essential crossings reflect the self-engulfing effect of the permanent entanglements which create the knot topology. If the knot is localized, the knot-graph approximation means that the chain within the knot region due to this self-engulfing effectively confines itself such that its entropy is expected to be comparable to the construct which emerges when the essential crossings are actually thought of as real contact points between the chain. That is, the resulting construct is a 3D paraknot, a polymer chain with 'slip-links' [14]. In other words, the *knot-graph assumption* states that, due to the localization of the knot, the number of degrees of freedom of this knot can effectively be obtained from a polymer network in which the topological entanglements are replaced by vertices (point-like contacts) which now connect different segments of the polymer, such that these segments are allowed to exchange length with each other. Physically, one could envisage such vertex slip-links as little rings enforcing pair contacts along the chain such that the chain can still slide freely through them and the segments created by the slip-links can exchange

† We denote a knot by the number of essential crossings C and a subscript enumerating the different types of knots with the same C. As a knot-graph is the same for all m types of a given C, it is denoted by $\mathcal{G}(C)$ only.

‡ The mean size $\langle\ell\rangle$ is defined as

$$\langle\ell\rangle = \frac{\int_a^L \ell p(\ell)\,\mathrm{d}\ell}{\int_a^L p(\ell)\,\mathrm{d}\ell}$$

where a is a short-distance cutoff determined by the lattice constant. Thus, $\langle\ell\rangle \sim L$ if $c < 1$, $\langle\ell\rangle \sim a^{c-1}L^{2-c}$ if $1 < c < 2$, and $\langle\ell\rangle \sim a$ if $c > 2$.

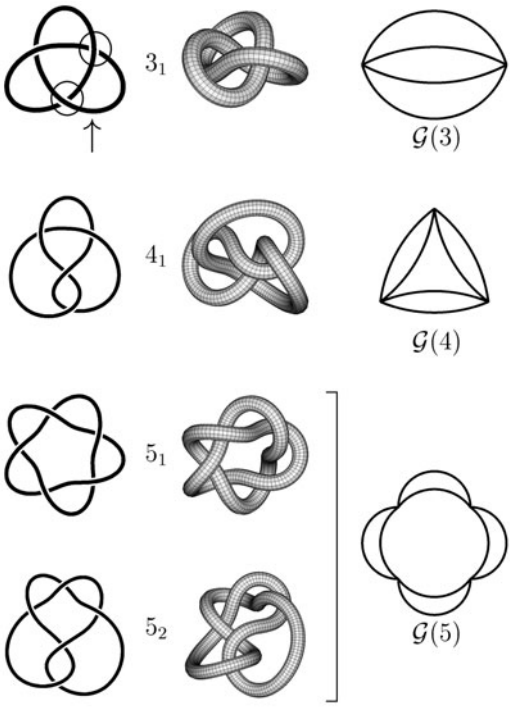

Figure 1. Normal projections (left) and 3D visualization (middle) of the knots 3_1, 4_1, 5_1 and 5_2, together with the associated knot-graphs $\mathcal{G}(C)$ (right) whose number of vertices is $n_4 = C - 1$, in terms of the number of essential crossings C of the knot. For 3_1, the arrow indicates the loop which is supposed to become the large one under the *a priori* assumption $L - \ell \gg \ell$; effectively, only one of the two associated vertices marked by the circles can be felt by the knot region with respect to the big loop for a given snapshot (i.e. the projection shows one crossing which effectively becomes irrelevant in the 3D configuration space). Similarly for the other knots.

length across these slip-link vertices. A subtlety arises in the actual number of such effective vertices, which are to be considered relevant for the knot-graph $\mathcal{G}(C)$ associated with a 3D knot C_m. We claim it is $C - 1$, again for the localized state we assumed. Observing the two circled crossings for the trefoil in figure 1, and assuming that the segment depicted by the arrow is the large, simply connected part of size $L - \ell$, it can be seen that only a negligible minority of configurations are realized such that both entanglements are actually enforced. This observation can be generalized for any knot which is localized, and it corresponds to the statement that a knot with C crossings can be represented by C polymer rings [15]†.

A justification for this second assumption, including the $C - 1$ choice for the number of effective vertices, comes from the studies of Quake who assumed in his analysis that a knot C_m can be decomposed into C independent loops. The predictions of this model were corroborated by numerical studies [15] and correspond to the results of the inflated sausage model of Grosberg *et al* [4, 17]. The difference to our model in Quake's approach lies only in the fact that for

† This argument appeals to one's 3D imagination, much as does the argument brought forth in [15] when arguing for the dissection of a knot C_m into C loops.

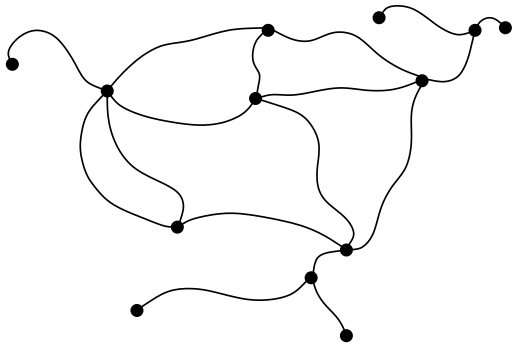

Figure 2. Polymer network $\mathcal{G}$ with vertices (●) of different order ($n_1 = 5$, $n_3 = 4$, $n_4 = 3$, $n_5 = 1$).

small chains all the rings are of approximately the same size, whereas in the long chain limit considered herein, they are of variable size such that the coupled fluctuations necessarily have to be considered. In fact, we will show that a knot-graph $\mathcal{G}(C)$ with $C - 1$ effective slip-link vertices corresponds exactly to C coupled loops.

To proceed, we recall that the configuration number of an arbitrary polymer network $\mathcal{G}$ with $\mathcal{N} = \frac{1}{2}\sum_{N\geq 1} N n_N$ segments of (fixed) length $s_1, s_2, \ldots, s_{\mathcal{N}}$, which are connected by the set of n_N vertices of order N, is [20]–[22]

$$\omega_{\mathcal{G}} \sim \mu^L s_{\mathcal{N}}^{\gamma_{\mathcal{G}}-1} \mathcal{Y}_{\mathcal{G}}\left(\frac{s_1}{s_{\mathcal{N}}}, \frac{s_2}{s_{\mathcal{N}}}, \ldots, \frac{s_{\mathcal{N}-1}}{s_{\mathcal{N}}}\right) \tag{1}$$

where $\mathcal{Y}_{\mathcal{G}}$ is a scaling function, and $\mathcal{L} = \frac{1}{2}\sum_{N\geq 1}(L-2)n_N + 1$ is the Euler number of physical loops; see also figure 2. μ is the (nonuniversal) connectivity constant of a self-avoiding walk, and the configuration exponent is $\gamma_{\mathcal{G}} = 1 - \mathcal{L}d\nu + \sum_{N\geq 1} n_N \sigma_N$, where σ_N are critical exponents designated to a junction (vertex) at which N legs of a self-avoiding walk are joined.

For the values of the critical exponents σ_N, there are two limiting cases: (i) one has hard vertices, i.e. the effective vertices in a knot-graph are considered real vertices in the polymer network sense at which N legs of a self-avoiding polygon meet; in particular, $\sigma_{N\geq 3} < 0$ [20]. This is a highly improbable scenario as, due to the magnitude, σ_N would lead to a maximally punished (smallest possible) $\omega_{\mathcal{G}(C)}$. The other extreme is the limit of (ii) soft vertices, i.e. keeping in mind that the knot-graph is only an effective representation of the knot, it is assumed that the topological exponents vanish,

$$\sigma_N \approx 0; \tag{2}$$

i.e. the tendency in a 3D knot is that two portions of the polymer, albeit held close by each other through the permanent topological entanglements, avoid direct contact with each other for self-avoiding effects. If the knot region is not too small, there are sufficient degrees of freedom left to assume that the topological exponents which usually quantify the *penalty* of bringing several legs of a self-avoiding polygon together in a vertex become *negligible*. That is, although different segments are close and effectively act like a vertex network, they will still tend to keep a minimum distance between each other to avoid penalties from the self-avoiding interaction. We will now show that this phenomenological knot-graph model fulfils all conditions self-consistently and is in good agreement with an exponent recently obtained for the 3D trefoil.

For the original trefoil graph, we observe two vertices of order 4, or $\mathcal{L} = 3$ physical loops, thus

$$\omega'_{\mathcal{G}(3)} \sim \mu^L (L-\ell)^{-3d\nu} \mathcal{Y}_{\mathcal{G}(3)}\left(\frac{s_1}{L-\ell}, \frac{s_2}{L-\ell}, \frac{s_3}{L-\ell}\right), \tag{3}$$

where the prime indicates that we keep the individual segments fixed. In our *a priori* assumption that $L - \ell \gg \ell$, the big ring segment should not be perceptibly influenced by the vicinal small-knot region. Thus, the expected exponent of the factor $(L-\ell)$ should be $-d\nu$, the well known loop closure exponent for a self-avoiding loop [12]. This determines the scaling behaviour of the first argument of the scaling function. Moreover, as the individual segments in the knot region can actually exchange length and thereby create additional degrees of freedom, we can integrate them out and obtain the following result (compare [12, 14]):

$$\omega_{\mathcal{G}(3)} \sim \mu^L (L-\ell)^{-d\nu} \ell^{-c_{\mathcal{G}(3)}}, \qquad c_{\mathcal{G}(3)} = 2d\nu - 2 \approx 1.528. \tag{4}$$

This implies

$$\langle \ell \rangle \sim a^{0.528} L^{0.472}, \tag{5}$$

i.e. weak localization (in the sense that $\langle \ell \rangle$ grows with L, but $\lim_{L\to\infty} \langle \ell \rangle / L = 0$). In particular, this renders the procedure following the *a priori* assumption $\ell \ll L - \ell$ self-consistent, *a posteriori*, see in more detail in what follows. The result (5) is remarkably close to the scaling $L^{0.4\pm0.1}$ reported by Farago *et al* [23] in force–extension simulations of a trefoil knot.

As shown for flat knots in [12], there exist contractions of the original configuration of such a graph in which one or more of the segments become so small that on the level of the scaling approach the vertices connected by such segments can no longer be resolved and are considered coalesced. The resulting configurations exhibit different scaling exponents c, which define a hierarchy of likely shapes of the network. For 3_1 and 4_1, the hierarchy of contractions and the associated exponents are shown in figure 3. For both, the leading order is taken by the original configuration, in contrast to the 2D case (with non-trivial σ_N) where the figure-eight structure leads the hierarchy of every prime knot [12]. In fact, from the general localization exponent

$$c = (\mathcal{L}-1)d\nu - (\mathcal{N}-2) = 2 - \sum_{N\geq 1} n_N \left(\frac{N}{2} - \left[\frac{N}{2} - 1\right] d\nu\right) \tag{6}$$

of a 3D network with $\sigma_N = 0$, it can be seen that the minimum value of c, and therefore the most likely contraction, is achieved for configurations with the maximum number of four-vertices (in our hierarchies, only vertices of even order and $N \geq 4$ occur)—but this corresponds exactly with the original knot-graph; for these leading shapes with n_4 four-vertices, expression (6) simplifies to

$$c = 2 - 0.236 n_4, \tag{7}$$

such that $c > 1$ holds exclusively for $n_4 \leq 4$: only knots with five essential crossings or less localize within our model. For more complex knots, our procedure (both the map to a knot-graph and the determination of c from the scaling function) is no longer self-consistent, and we expect delocalization for such more complex knots. Conversely, the weak localization found for simple knots ensures that:

(i) a confined knot region exists and therefore the map to a knot-graph is meaningful (*a priori* and knot-graph assumptions), and

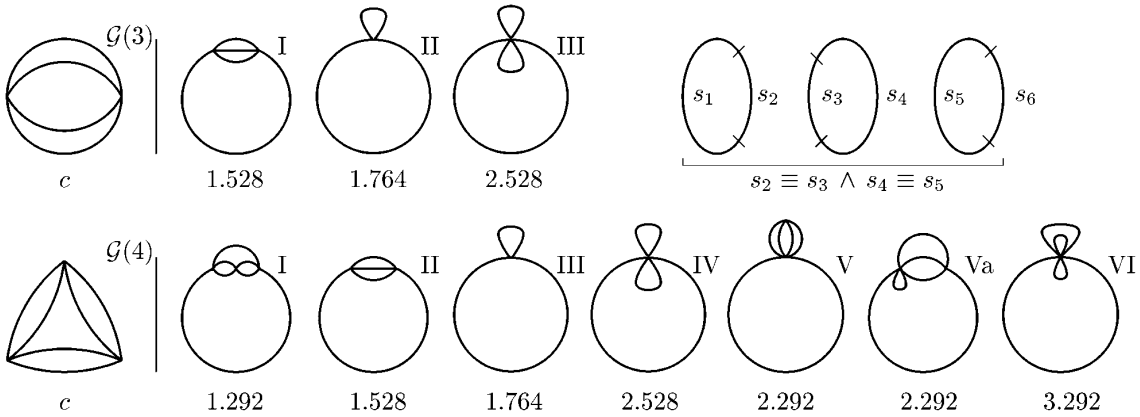

Figure 3. Knot graphs $\mathcal{G}(3)$ and $\mathcal{G}(4)$ with their hierarchies of contractions. Below each contraction, the associated localization exponent c is given. For $\mathcal{G}(3)$, the corresponding three-loop representation is shown on the right, indicating the constraints. For higher order knots, the corresponding graph $\mathcal{G}(C)$ corresponds to $C-1$ loops around a central loop, as becomes obvious from the configuration number results (4) and (6). The constraints, which couple individual segment lengths, reflect the self-embracing nature of knots, i.e. that one loop engulfs another.

(ii) the knot of size $\langle \ell \rangle \sim a^{c-1} L^{2-c}$ region contains sufficient degrees of freedom such that the different segments can still avoid coming too close to each other, i.e. to ensure the assumption $\sigma_N \approx 0$ (soft vertices assumption).

Thus, the knot-graph modelling of 3D knots is self-consistent in a delicate twofold sense.

3. Discussion

Compare our results with the decomposition model of knots into C independent, self-avoiding loops of length L/C used by Quake [15, 24]. As mentioned before, this model predicts that the average extension of the knot decreases with increasing complexity, as to $R_g^2 \sim AC^{1/3-\nu} L^{2\nu}$. In contrast, our model predicts that knots with $C \leq 5$ localize weakly, and to leading order their gyration radius is fully independent of C. Only for higher knots, delocalization effects are expected, leading to a behaviour of the prefactor A similar to Quake's result. Whereas the C-dependence of the simulations in [15] may be attributed to finite-size effects [19], the difference in the independent loop model advocated in [15] to our model suggested here lies in the coupling of loops: knot-graphs are equivalent to *coupled* self-avoiding loops, as is obvious from the corresponding expression for $\omega_{\mathcal{G}(C)}$ and the knot-graphs $\mathcal{G}(C)$ themselves (as $\sigma_N \equiv 0$). These loops exchange length and share some of the segment sizes, as illustrated for the trefoil graph in figure 3. In this sense, the knot-graph model is the natural complement to Quake's model in the long chain limit.

With respect to previous simulation results, we note that the localization behaviour is consistent with the results reported by Janse van Rensburg and Whittington [18], Orlandini *et al* [19], as well as with the peaks in the distribution of the size of the knot regions located at relatively small sizes reported by Katritch *et al* [10]. Only for the six-knot, for which [18]

and [19] find localization, a discrepancy seems to exist. However, since this case is exactly the first non-localizing knot in our model, it might be related to the approximative nature of our approach. It may well also be a borderline case in the numerical resolution of the results reported in [18, 19]. Conversely, there is no contradiction with the findings of Katritch *et al* [10], as a peak in the distribution of sizes of the knot region can occur even if the average size is proportional to L†.

Intuitively, one could try to model a knot in the ideal chain limit in terms of random walks which have to mutually return inside one another. However, this approach leads to equally distributed loop sizes in all dimensions. The model presented here, in contrast, leads to weak localization in dimensions above 4 for ideal chains, and it seems that the cooperatively acting closed loops grasp the self-embracing nature of knots better than the (unclosed) returning random walk picture.

Two major aspects are different from the results of the (exactly treatable) case of flat knots:

(i) 3D knot-graphs are not universal in the sense that only the simple knots localize at all, and each of these has a different leading shape in the associated hierarchy;

(ii) the trade-off between the degrees of freedom within the knot region and the segregated simple ring polymer is shifted towards the knot region.

This causes the interesting phenomenon that simple knots should be localized weakly, whereas more complex knots are expected to delocalize. Note, however, that the universality of both strong localization $\langle \ell \rangle \sim a$ and leading figure-eight contraction would pertain to 3D knots of any C, if the case of hard vertices was realized.

4. Conclusion

The strong localization ($\langle \ell \rangle \sim a$) found in flat (2D) knots and in simple paraknots in both two dimensions and three dimensions is brought about through the assistance of the topological exponents σ_N [12, 14]. They come into play as each N-vertex forces the legs of N self-avoiding walks close to each other. In contrast, in the model conjectured here, the weak localization still allows sufficient degrees of freedom for the knot region such that different segments can avoid coming too close to each other. As a consequence, the proposed map of 3D knots on effective vertex networks predicts weak localization for the knots 3_1, 4_1, 5_1 and 5_2, or composite knots whose prime components correspond to these, where the weak localization is caused by the loop closure exponents $d\nu$. All knots with a higher number of essential crossings are expected to delocalize. The leading order contribution within the associated hierarchy of contractions for $C \leq 5$ knots corresponds to the original knot network with the maximum number of σ_4-vertices. For the trefoil, the obtained value for c is in good agreement with the measured value reported by Farago *et al* [23]. In composite knots with simple prime components, the latter become statistically independent, weakly localized units around the central large loop, compare [12, 14]. The knot-graph approach is based on a delicate balance in the localization properties: the obtained weak localization, $\langle \ell \rangle \sim a^{c-1} L^{2-c}$ with $1 < c < 2$, gives rise to a confined knot region for $C \leq 5$; still, this region grows with L, such that the assumption of vanishing vertex exponents $\sigma_N \approx 0$ becomes reasonable.

† Even if the mean size of the 'knot region' grows linearly with the system size, a typical configuration might still be asymmetric, as for the constructed probability density function $p(\ell, L-\ell) \sim \ell^{-3/4}(L-\ell)^{-3/4}$. Here, p is peaked in the corners $\ell \to 0$ and $\to L$, and at the same time $\langle \ell \rangle \sim L$ (compare [12, 14]).

Let us put these results into perspective with the knot detection problem in long biological DNA†. If the knot is simple (as most of the reported DNA knots are) our model predicts weak localization in the long-chain limit. Even if finite-size effects come into play (the persistence length of a double-helix is roughly 500 Å) there should remain an entropy-caused asymmetry between the knot region and the remaining part of the DNA which, in turn, may be enough to enable the knot detection through topoisomerases, as predicted by the models in [6]. For electrophoresis motility assays of DNA chains, it is expected that simple knots in long enough chains should exhibit no motility dependence on the knot type (see footnote on previous page). To actually quantify what a long chain in that context is may strongly depend on the environmental conditions such as salt content.

Our approach to map 3D knots on knot-graphs is certainly an approximation. On the one hand, the assumption that the topological exponents vanish, $\sigma_N \approx 0$, in a 3D knot may well be taken for granted. This is due to the existing degrees of freedom of the knot in its 3D embedding, which allows the segments to avoid coming into direct contact, and therefore avoid penalties from self-avoiding interactions. Furthermore, the claim that a knot-graph comprises $C - 1$ vertices is consistent with previous modelling approaches. On the other hand, the phenomenological mapping on a polymer network with effective vertices is an interpretation of both the results for the flat knots as well as the symmetries indicated in the knot projection, fuelled by the fact that in a weakly localized knot region the different segments are automatically close to each other. This being said, we believe that this (self-consistent!) model gives rise to rich and interesting predictions which may stimulate further investigations in simulation studies; in particular, the simulation study of the localization behaviour of 3D knots with $C \gtrsim 6$. Similarly, motility assays for longer chains could possibly distinguish the qualitatively different behaviour of $C \leq 5$ and higher knots. Finally, it is hoped that it may instigate a more direct analytical approach to the mutually engulfing, self-embracing nature of knots and other permanent entanglements in single and multichain systems.

Acknowledgments

The author is happy to acknowledge helpful discussions with Mehran Kardar, Yacov Kantor, Andreas Hanke and Paul G Dommersnes. RM acknowledges partial funding by the Deutsche Forschungsgemeinschaft within the Emmy Noether programme.

References

[1] Frisch H L and Wasserman E 1961 *J. Am. Chem. Soc.* **83** 3789
Delbrück M 1962 Mathematical problems in the biological sciences *Proc. Symp. Appl. Math.* vol 14, ed R E Bellman p 55
[2] Sumners D W and Whittington S G 1988 *J. Phys. A: Math. Gen.* **21** 1689
Pippenger N 1989 *Discrete Appl. Math.* **25** 273
[3] Dobay A, Sottas P E, Dubochet J and Stasiak A 2001 *Lett. Math. Phys.* **55** 239
Koniaris K and Muthukumar M 1991 *Phys. Rev. Lett.* **66** 2211
The characteristic chain length N_0 may become surprisingly long; see, e.g.,

† For very short DNA, in contrast, the effect of the persistence length will cause the different segments to exert a force on the confining entanglements and thus enable easier detection, much as it is believed to work in the entanglement-removal during chromosome division in eukaryotes [5].

Shimamura M and Deguchi T 2000 *Phys. Lett.* A **274** 184
Grosberg A 2002 *Preprint* cond-mat/0207427
[4] Grosberg A Yu 2000 *Phys. Rev. Lett.* **85** 3858
[5] Alberts B, Roberts K, Bray D, Lewis J, Raff M and Watson J D 1994 *The Molecular Biology of the Cell* (New York: Garland)
Bolsover S R, Hyams J S, Jones S, Shephard E A and White H A 1997 *From Genes to Cells* (New York: Wiley)
[6] Wasserman S A, Dungan J M and Cozzarelli N R 1985 *Science* **229** 171
Shaw S Y and Wang J C 1993 *Science* **260** 533
Sogo J M, Stasiak A, Martinez-Robles M L, Krimer D B, Hernandez P, and Schvartzman J B 1999 *J. Mol. Biol.* **286** 637
[7] Strick T R, Croquette V and Bensimon D 2000 *Nature* **404** 901
Rybenkov V V, Ullsperger C, Vologodskii A V, and Cozzarelli N R 1997 *Science* **277** 690
Yan J, Magnasco M O and Marko J F 1999 *Nature* **401** 932
Vologodskii A V, Zhang W T, Rybenkov V V, Podtelezhnikov A A, Subramanian D, Griffith J D and Cozzarelli N R 2001 *Proc. Natl Acad. Sci. USA* **98** 3045
[8] Sauvage J-P and Dietrich-Buchecker C 1999 *Molecular Catenanes, Rotaxanes, and Knots: A Journey Through the World of Molecular Topology* (Weinheim: VCH)
Lehn J-M 1995 *Supramolecular Chemistry* (Weinheim: VCH)
[9] Hanke A and Metzler R 2002 *Chem. Phys. Lett.* **359** 22
[10] Katritch V, Olson W K, Vologodskii A, Dubochet J and Stasiak A 2000 *Phys. Rev.* E **61** 5545
[11] Guitter E and Orlandini E 1999 *J. Phys. A: Math. Gen.* **32** 1359
[12] Metzler R, Hanke A, Dommersnes P G, Kantor Y and Kardar M 2002 *Phys. Rev. Lett.* **88** 188101
[13] Kauffman L H 1993 *Knots and Physics* (Singapore: World Scientific)
[14] Metzler R, Hanke A, Dommersnes P G, Kantor Y and Kardar M 2002 *Phys. Rev.* E **65** 061103
[15] Quake S R 1994 *Phys. Rev. Lett.* **73** 3317
Quake S R 1986 *Phys. Rev.* E **52** 1176
[16] Shaw S Y and Wang J C 1993 *Science* **260** 533
Stasiak A, Katritch V, Bednar J, Michoud D and Dubochet J 1996 *Nature* **384** 122
Vologodskij A V, Crisona N J, Laurie B, Pieransku P, Katritch V, Dubochet J and Stasiak A 1998 *J. Mol. Biol.* **278** 1
[17] Grosberg A Yu, Feigel A and Rabin Y 1996 *Phys. Rev.* E **54** 6618
[18] Janse van Rensburg E J and Whittington S G 1991 *Phys. Rev.* E **54** 3935
[19] Orlandini E, Tesi M C, Janse van Rensburg E J and Whittington S G 1998 *J. Phys. A: Math. Gen.* **31** 5953
[20] Duplantier B 1986 *Phys. Rev. Lett.* **57** 941
Duplantier B 1989 *J. Stat. Phys.* **54** 581
[21] Schäfer L, Ferber C v, Lehr U and Duplantier B 1992 *Nucl. Phys.* B **374** 473
[22] Ohno K and Binder K 1988 *J. Physique* **49** 1329
[23] Farago O, Kantor Y and Kardar M 2002 *Preprint* cond-mat/0205111
[24] Compare also to the decomposition of the trefoil knot region into repelling, fluctuating, Gaussian loops in Ben-Naim E, Daya Z A, Vorobieff P and Ecke R E 2001 *Phys. Rev. Lett.* **86** 1414